
Consistency Model is an Effective Posterior Sample Approximation for Diffusion Inverse Solvers

Tongda Xu, Ziran Zhu, Jian Li, Dailan He, Yuanyuan Wang, Ming Sun
Tsinghua University, SenseTime Research
x.tongda@nyu.edu

Ling Li, Hongwei Qin, Yan Wang, Jingjing Liu, Ya-Qin Zhang
Kuaishou Technology, Chinese Academy of Sciences
wangyan@air.tsinghua.edu.cn

Abstract

Diffusion Inverse Solvers (DIS) are designed to sample from the conditional distribution $p_\theta(X_0|y)$, with a predefined diffusion model $p_\theta(X_0)$, an operator $f(\cdot)$, and a measurement $y = f(x'_0)$ derived from an unknown image x'_0 . Existing DIS estimate the conditional score function by evaluating $f(\cdot)$ with an approximated posterior sample drawn from $p_\theta(X_0|X_t)$. However, most prior approximations rely on the posterior means, which may not lie in the support of the image distribution, thereby potentially diverge from the appearance of genuine images. Such out-of-support samples may significantly degrade the performance of the operator $f(\cdot)$, particularly when it is a neural network. In this paper, we introduce a novel approach for posterior approximation that guarantees to generate valid samples within the support of the image distribution, and also enhances the compatibility with neural network-based operators $f(\cdot)$. We first demonstrate that the solution of the Probability Flow Ordinary Differential Equation (PF-ODE) with an initial value x_t yields an effective posterior sample $p_\theta(X_0|X_t = x_t)$. Based on this observation, we adopt the Consistency Model (CM), which is distilled from PF-ODE, for posterior sampling. Furthermore, we design a novel family of DIS using only CM. Through extensive experiments, we show that our proposed method for posterior sample approximation substantially enhances the effectiveness of DIS for neural network operators $f(\cdot)$ (e.g., in semantic segmentation). Additionally, our experiments demonstrate the effectiveness of the new CM-based inversion techniques. The source code is provided in the supplementary material.

1 Introduction

Diffusion inverse solvers (DIS) are a family of algorithms that solve the inverse problem using diffusion prior [Li et al., 2023, Moser et al., 2024]. More specifically, given an operator $f(\cdot)$, a measurement $y = f(x'_0)$ from some unknown image x'_0 , and a diffusion model $p_\theta(X_0)$, DIS aim to sample from the conditional distribution $x_0 \sim p_\theta(X_0|y)$. For example, when $f(\cdot)$ is a down-sampling operator, DIS is a perceptual super-resolution algorithm [Menon et al., 2020]. However, we cannot sample from $p_\theta(X_0|y)$ directly as it is intractable. To tackle this challenge, previous works adopt a variety of techniques such as linear projection [Wang et al., 2022, Kawar et al., 2022, Chung et al., 2022b, Lugmayr et al., 2022, Song et al., 2022, Pokle et al., 2024, Cardoso et al., 2024], variational inference [Feng et al., 2023, Mardani et al., 2023, Janati et al., 2024], Bayesian filter [Dou and Song, 2023], sequential Monte Carlo [Wu et al., 2024, Phillips et al., 2024], proximal gradient [Xu and Chi, 2024] and conditional score estimation [Chung et al., 2022a, Yu et al., 2023, Zhu et al., 2023, He et al., 2023c, Song et al., 2023b, Boys et al., 2023, Rout et al., 2023, 2024] for approximate or exact sampling.

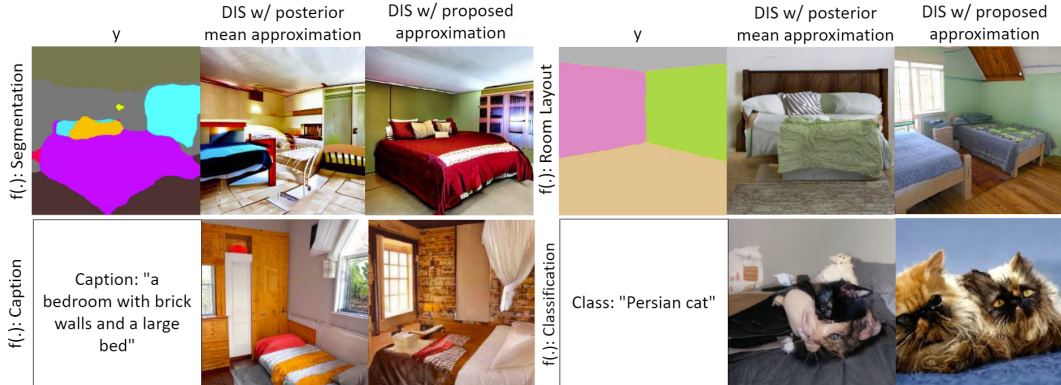


Figure 1: A visual comparison of DIS with posterior mean as approximation for posterior sample, and DIS with proposed CM approximation for posterior sample.

Among those DIS techniques, the conditional score estimation methods [Chung et al., 2022a, Song et al., 2023c] are most widely adopted, as they are suitable for general non-linear, noisy operator $f(\cdot)$ and quite efficient in practice. During the inverse diffusion process from X_T to X_0 , they estimate the conditional score $\nabla_x \log p_\theta(X_t|y)$ by evaluating operator $f(\cdot)$ with posterior sample from $p_\theta(X_0|X_t)$. As the posterior $p_\theta(X_0|X_t)$ is generally intractable, various approximations to posterior sample are proposed based on posterior mean: they either directly adopt posterior mean [Chung et al., 2022a, Yu et al., 2023, Zhu et al., 2023, He et al., 2023c] or construct a uni-modal distribution centered at posterior mean [Song et al., 2023b, Boys et al., 2023, Rout et al., 2023, 2024].

However, those posterior-mean based approximate posterior samples are far from real images, as it is well-known that the mean of noisy images may not lie in the support of the image distribution [Ledig et al., 2017, Blau and Michaeli, 2018]. Although those out-of-distribution approximations are shown to be successful for simple $f(\cdot)$ such as down-sampling and motion blurring, they might fail for more complex $f(\cdot)$, especially when $f(\cdot)$ are neural networks such as segmentation or classification, which are sensitive to out-of-distribution inputs.

In this paper, we propose a novel approach to approximate posterior sample for DIS. Our approximations are guaranteed to be valid images and generally perform well for neural network $f(\cdot)$. More specifically, we first show that given initial condition $X_t = x_t$, the solution of probability flow ordinary differential equation (PF-ODE) [Song et al., 2020] is a valid posterior sample of true posterior $p_\theta(X_0|X_t = x_t)$. Inspired by this, we propose to use consistency model (CM), a distillation of PF-ODE as a posterior sample approximation for DIS. Furthermore, we propose a new family of DIS by iteratively inverting CM in a generative adversarial network (GAN) inversion fashion [Creswell and Bharath, 2016, Menon et al., 2020]. Empirically, by using CM as posterior sample approximation, we improve the DIS’s performance when operators are neural networks, such as semantic segmentation and image captioning. Furthermore, our experiments demonstrate the CM inversion also performs well for both neural network and non-neural network operators.

2 Preliminaries

2.1 Diffusion Model

Diffusion model is a type of generative model with T steps Gaussian Markovian chain in continuous space [Sohl-Dickstein et al., 2015]. Two widely adopted diffusion models are variance preserving (VP) and variance exploding (VE) diffusion. We follow the formulation of VE diffusion [Song et al., 2020], and refer VP diffusion to Ho et al. [2020], Kingma et al. [2021]. We denote the source image as X_0 , and the forward process of VE diffusion is a Markov chain:

$$q(X_T, \dots, X_1|X_0) = \prod_{t=1}^T q(X_t|X_{t-1}), \text{ where } q(X_t|X_{t-1}) = \mathcal{N}(X_t - \sigma_t^2 X_{t-1}, (\sigma_t^2 - \sigma_{t-1}^2)I), \quad (1)$$

where σ_t^2 are hyper-parameters (typically called variance schedule). The reverse diffusion process is also a Markov chain, with transition kernel $p(X_{t-1}|X_t)$ depending on the score function $\nabla_{X_t} \log p(X_t)$. To learn such a diffusion model, one can use a neural network $s_\theta(t, X_t)$ (parametrized by θ) to match the score function $\nabla_{X_t} \log p(X_t)$, and the resulting reverse diffusion process is given by

$$p_\theta(X_0, \dots, X_T) = p(X_T) \prod_{t=1}^T p_\theta(X_{t-1}|X_t),$$

where $p_\theta(X_{t-1}|X_t) = \mathcal{N}(X_t + (\sigma_t^2 - \sigma_{t-1}^2)s_\theta(t, X_t), (\sigma_t^2 - \sigma_{t-1}^2)I)$. (2)

Song et al. [2020] show that the reverse diffusion can be seen as a discretization of reverse stochastic differential equation (SDE) [Anderson, 1982]. Further, there exists a probability flow ordinary differential equation (PF-ODE) that has the same marginal distribution $p_\theta(X_t)$ as the reverse SDE:

$$\begin{aligned} \text{reverse SDE: } dX_t &= -\frac{d\sigma_t^2}{d_t} s_\theta(t, X_t) dt + \sqrt{\frac{d\sigma_t^2}{d_t}} dB_t \quad \xleftrightarrow{\text{same } p_\theta(X_t)} \\ \text{PF-ODE: } dX_t &= -\frac{1}{2} \frac{d\sigma_t^2}{dt} s_\theta(t, X_t) dt, \end{aligned} \quad (3)$$

where B_t is the standard Brownian motion. Therefore, solving either of them is equivalent to sampling from the reverse diffusion process. Another useful result is Tweedie’s formula [Efron, 2011], which provides an efficient estimation to the mean of posterior $p_\theta(X_0|X_t)$:

$$\mathbb{E}[X_0|X_t] = X_t + \sigma_t^2 s_\theta(t, X_t). \quad (4)$$

2.2 Diffusion Inverse Solvers with Conditional Score Estimation

Given an operator $f(\cdot)$, a target measurement $y = f(x'_0)$ from an unknown x'_0 and a diffusion model $p_\theta(X_0)$, the diffusion inverse solvers (DIS) attempt to sample from the conditional distribution $p_\theta(X_0|y)$. In this paper, we focus on DIS with conditional score estimation [Chung et al., 2022a, Song et al., 2023b]. More specifically, this paradigm of DIS attempts to estimate the conditional score $\nabla_{X_t} \log p_\theta(X_t|y)$. With this conditional score at hand, sampling from $p_\theta(X_0|y)$ is as easy as solving the reverse SDE or PF-ODE in Eq. 3 with $s_\theta(t, X_t)$ replaced by the conditional score.

More specifically, Chung et al. [2022a], Song et al. [2023c] propose to expand the conditional score into unconditional score and a term that is related to a distance $d(f(x_{0|t}), y)$, where $x_{0|t}$ is the sample from posterior $p_\theta(X_0|X_t)$ and $d(\cdot, \cdot)$ is a distance:

$$\begin{aligned} \nabla_{X_t} \log p_\theta(X_t|y) &= \nabla_{X_t} \log p_\theta(y|X_t) + \nabla_{X_t} \log p_\theta(X_t), \\ \nabla_{X_t} \log p_\theta(y|X_t) &= \nabla_{X_t} \log \mathbb{E}_{p_\theta(X_0|X_t)} [p_\theta(y|X_0)] \approx \nabla_{X_t} \log \sum_{\substack{i=1, \dots, K \\ x_{0|t}^{(i)} \sim p_\theta(X_0|X_t)}} p_\theta(y|X_0 = x_{0|t}^{(i)}), \\ p_\theta(y|X_0 = x_{0|t}^{(i)}) &\propto \exp -d(f(x_{0|t}^{(i)}), y). \end{aligned} \quad (5)$$

Under this formulation, an important issue is how to effectively draw differentiable samples from posterior $p_\theta(X_0|X_t)$. Obviously, direct ancestral sampling from reverse diffusion is computationally expensive. Chung et al. [2022a] propose to use the posterior mean computed by Tweedie’s formula in Eq. 4 as the posterior sample. Song et al. [2022, 2023b] propose to model the posterior as a Gaussian distribution with mean being the posterior mean as mean and the covariance chosen as a hyper-parameter. Rout et al. [2023], Boys et al. [2023] improve Song et al. [2022, 2023b] by using the posterior covariance computed by second order Tweedie’s formula as the covariance of Gaussian. There are several other approaches that follow conditional score estimation paradigm [Yu et al., 2023, Chung et al., 2023, Song et al., 2023a, He et al., 2023b, Rout et al., 2024, Meng and Kabashima, 2022, Dou and Song, 2023, Chung et al., 2022b, Song et al., 2022, He et al., 2023a] and rely on those approximations.

3 Consistency Model is an Effective Posterior Sample Approximation for DIS

3.1 Previous Approximations are Out-of-Distribution

Most previous approximations to $p_\theta(X_0|X_t)$ either directly use the posterior mean or construct a uni-modal distribution entered around the posterior mean. However, the posterior mean $\mathbb{E}[X_0|X_t]$ is a mean-square error (MSE) minimizer for images perturbed by Gaussian noise, which does not necessarily correspond to a valid image [Ledig et al., 2017, Blau and Michaeli, 2018]. In other words, the posterior mean may not lie in the support of natural image distribution, leading to its density in both marginal and posterior distributions approaching zero.:

$$p_\theta(X_0 = \mathbb{E}[X_0|X_t = x_t]) \approx 0, p_\theta(X_0 = \mathbb{E}[X_0|X_t = x_t]|X_t = x_t) \approx 0 \quad (6)$$

When the operator is a neural network, such out-of-distribution approximations can significantly

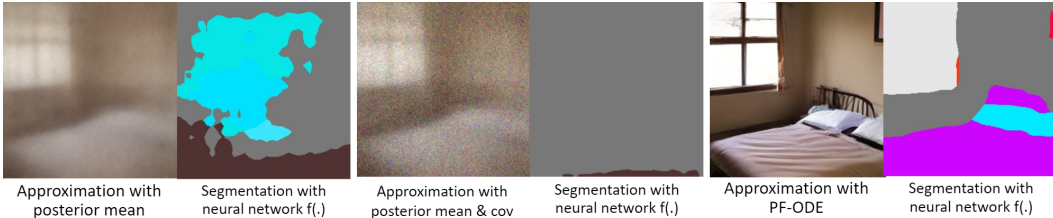


Figure 2: Different approximations of posterior sample, and their output after a segmentation $f(\cdot)$.

degrade the sample quality. A visual example is shown in Fig. 2. The approximation using posterior mean, and the approximation using Gaussian centered at the posterior mean are not valid image samples. Consequently, when these approximations are processed through a semantic segmentation operator $f(\cdot)$, the outputs are nonsensical.

3.2 PF-ODE provides an Effective Posterior Sample Approximation

It is known that the PF-ODE and reverse SDE in Eq. 3 have the same marginal distribution, which is the image distribution $p_\theta(X_0)$ if the score is learned perfectly [Song et al., 2020]. Denote the solution of PF-ODE given initial condition $X_t = x_t$ as $\Phi_0(x_t)$, then this solution is in support of natural image distribution, and the density of the solution is non-zero:

$$p_\theta(X_0 = \Phi_0(x_t)) > 0. \quad (7)$$

Back to the previous example in Fig. 2, when using PF-ODE as posterior sample approximation, the semantic segmentation operator $f(\cdot)$ produces reasonable result. However, knowing $p_\theta(X_0 = \Phi_0(x_t)) > 0$ is not enough. As we are seeking a posterior sample approximation, we need to ensure the solution $\Phi_0(x_t)$ has positive density on the posterior distribution, *i.e.*, $p_\theta(X_0 = \Phi_0(x_t)|X_t = x_t) > 0$.

To the best of our knowledge, the relationship between PF-ODE’s solution $\Phi_0(x_t)$ given initial value $X_t = x_t$, and the posterior $p_\theta(X_0|X_t = x_t)$ is not well understood. In this section, we show that the solution of PF-ODE has non-zero density in true posterior for any time t , *i.e.*,

$$\forall x_t, p_\theta(X_0 = \Phi_0(x_t)|X_t = x_t) > 0. \quad (8)$$

Assumption 3.1. We assume the following conditions hold:

- The distribution $p_\theta(X_0)$ can be approximated by a d -dimension Gaussian Mixture Model (GMM) composed of N Gaussians with same small diagonal covariance $\sigma^2 I$ and mean μ^i :

$$p_\theta(X_0) \approx \frac{1}{N} \sum_{i=1}^N \mathcal{N}(X_0|\mu^i, \sigma^2 I). \quad (9)$$

- The solution $\Phi_0(x_t)$ and initial value x_t are bounded, *i.e.*, $\|\Phi_0(x_t)\| < c, \|x_t\| \leq c$.

- As PF-ODE is margin preserving and the dimension of data is high, the solution of PF-ODE is close to the surface of a sphere centered at μ^i with radius $\sqrt{d}\sigma$ [Vershynin, 2018], i.e., $\exists k, \text{ s.t. } \|\Phi_0(x_t) - \mu^k\|^2 \leq \sigma^2 + d\sigma^2$ with probability $1 - p$ for small p .

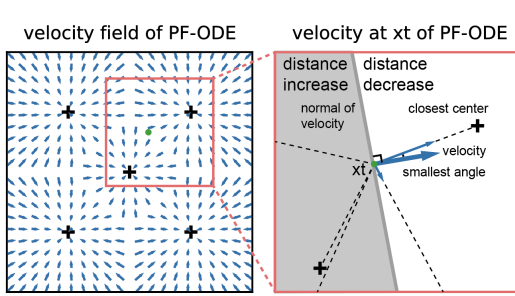
Proposition 3.2. *The solution of PF-ODE has a positive likelihood in true posterior with high probability, i.e.,*

$$p_\theta(X_0 = \Phi(x_t)|X_t = x_t) \geq \frac{1}{N} \frac{1}{\sqrt{(4\pi\sigma^2)^d}} \exp\left(-\frac{2c^2}{\sigma_t^2} - \frac{d+1}{2}\right), \text{ with probability } 1 - p. \quad (10)$$

Despite the solution of PF-ODE has a non-zero density in true posterior with high probability, we can not tell whether the solution falls into the highest density mode of true posterior. However, when σ_t^2 is small, we can show that the solution of PF-ODE is approximately the highest density mode of true posterior.

Lemma 3.3. *The PF-ODE can be written as:*

$$\frac{dX_t}{dt} = \underbrace{\sum_{i=1}^N \frac{w_i}{2} \frac{d\sigma_t^2}{dt} (X_t - \mu^i)}_{\text{velocity field } v_t}, w_i = \left(\exp - \frac{\|X_t - \mu^i\|^2}{2(\sigma^2 + \sigma_t^2)}\right) / \left(\sum_{j=1}^N \exp - \frac{\|X_t - \mu^j\|^2}{2(\sigma^2 + \sigma_t^2)}\right). \quad (11)$$



We can consider the velocity field v_t of PF-ODE in Eq. 11. The velocity field is a sum of vectors pointing to centers μ^i weighted by soft-max function w_i . When t is small, w_i becomes a "hard"-max which selects the closest center μ^* to initial point x_t , and the velocity field always points to μ^* . On the other hand, this closest center μ^* is also the highest density mode in true posterior (See Appendix. A). With this coincidence, the solution of PF-ODE with $X_t = x_t$ is approximately the mode with highest density in true posterior.

Figure 3: The PF-ODE's velocity field of a five GMM example.

When σ_t^2 is not small enough, we can still consider other conditions when PF-ODE will converge to the closest center μ^* . Consider the five GMM example in Figure. 3 with initial point $X_t = x_t$. An obvious intuition is that the normal plane of velocity v_t divide the space into two parts. In one part, the velocity has a negative projection on center's direction. In the other part, the velocity has a positive projection. Then, X_t will move away from the centers with negative projection, to the centers with positive projection. Among the centers with positive projection, when the closest center μ^* also has the smallest angle with velocity, it is very likely that the PF-ODE eventually converges into the closest center.

3.3 A Toy Example

To better understand the results above, we provide a toy example in \mathbb{R}^2 . As shown in Fig. 4, the source distribution $p(X_0)$ is a five Gaussian mixture model (GMM). Each Gaussian is diagonal with standard deviation $\sigma_0 = 0.1$. The centers of Gaussians are $(-1, -1), (-1, 1), (1, 1), (1, -1), (0, 0)$. We adopt VE diffusion with $\sigma_T = 4, T = 100$ and σ schedule in Karras et al. [2022]. The score function $\nabla_{X_t} \log p(X_t)$ is computed analytically.

As shown in Fig. 4.upper, starting from $x_t = (1, 0.4)$, the posterior $p(X_0|X_t = x_t)$ has most density on two right-hand side Gaussians. However, the approximation with posterior mean is close to $(1, 0.4)$, where true posterior has almost no density. Furthermore, the approximation with posterior mean and covariance also concentrates on a region where true posterior has almost no density. However, the approximation with PF-ODE falls into a high density region of true posterior.

We also visualize the highest density mode's decision boundary of true posterior and PF-ODE starting at different σ_t^2 . As shown in Fig. 4.lower, the decision boundary of true posterior is always a Voronoi cell centered at μ^i . When σ_t^2 is small, the solution of PF-ODE is similar to the true posterior. As σ_t^2 increase, the solution of PF-ODE becomes less similar to true posterior. However, at that time, the density scatters more evenly in the true posterior. The solution of PF-ODE still has non-zero density.

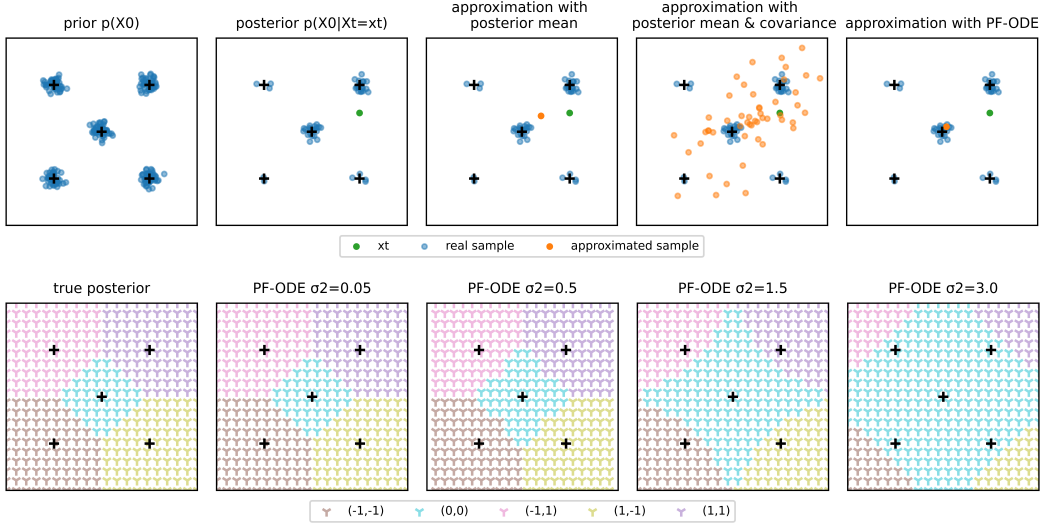


Figure 4: A toy example with five GMM.

3.4 Implementation of PF-ODE Approximation with Consistency Model

Directly solving PF-ODE is also intractable for DIS. Fortunately, PF-ODE can be distilled by Consistency Model (CM) [Song et al., 2023c]. More specifically, CM trains a one-step neural function $g_\theta(t, x_t)$ to approximate the solution of PF-ODE $\Phi_0(x_t)$. Its gradient is cheap to evaluate. Therefore, we can directly replace the $x_{0|t} \sim p_\theta(X_0|X_t = x_t)$ step in Eq. 5 by $x_{0|t} = g_\theta(t, x_t)$.

In practice, we find CM often over-fits the operator $f(\cdot)$. More specifically, the CM approximated sample $x_{0|t}$ is numerically close to y after passing the operator $f(\cdot)$. However, by inspecting $x_{0|t}$ visually, one often concludes that it is not aligned with y . (See an example in Fig. 6).

In fact, the resulting overfitted sample is an adversarial example [Szegedy et al., 2013], which is aligned with label y according to neural network but not aligned with y according to human eye. To make $f(\cdot)$ robust, we propose to add a small Gaussian noise to the output of CM as literature in adversarial robustness [Li et al., 2019]

$$x_{0|t} = g_\theta(t, x_t) + \mathcal{N}(0, \tau^2). \quad (12)$$

3.5 Consistency Model Inversion

We have shown that CM can be used as posterior sample approximator for DIS. As CM can be seen as a conditional GAN conditioned on timestep t and state x_t , a natural question to ask is: can CM be inverted in a GAN inversion fashion [Creswell and Bharath, 2016, Menon et al., 2020]?

We first review GAN inversion briefly. GAN inversion optimizes the noise z by penalizing the distance between generated image and the target for K steps. And step by step, the optimized z will generate an image that satisfies the constraint. Denote $h_\theta(\cdot)$ as GAN, we have

$$z^0 \sim \mathcal{N}(0, I), x^i = h_\theta(z^i), z^{i+1} = z^i - \zeta \frac{d}{dz^i} d(f(x^i), y), i = 0, \dots, K - 1. \quad (13)$$

Recall that CM first initializes an x_T from Gaussian distribution, then transforms it into target image $x_{0|t}$ by a neural network. Then iteratively CM adds a small noise back to $x_{0|t}$ and denoises again. For each iteration, CM is the same as GAN. To CM, for each iteration, we can invert CM as GAN inversion. In other words, we can stack several GAN inversions together, according to the iterative CM sampling algorithm in Algorithm 7, to obtain our final CM inversion algorithm in Algorithm 8. For each iteration, a GAN inversion is performed. Similarly, we also find that adding a small Gaussian noise is beneficial to neural-network $f(\cdot)$.

4 Experiments

4.1 Experiment Setup

Base Diffusion Models For diffusion model, we use a pretrained VE diffusion - EDM [Karras et al., 2022] provided by Song et al. [2023c]. For EDM-related methods, we adopt ancestral sampler with 1000 Euler steps. For CM [Song et al., 2023c], we employ the official pre-trained model by Song et al. [2023c]. The details are shown in Appendix. B.

Operators We evaluate all the methods with four neural network operators: semantic segmentation, room layout estimation, image captioning and image classification. For layout estimation, we adopt the neural network by Lin et al. [2018]. For semantic segmentation, we use the neural network by Zhou et al. [2017]. For image captioning, we employ BLIP [Li et al., 2022]. For image classification, we use ResNet [He et al., 2015]. In addition, we also evaluate a simple non-neural network operator: down-sampling (x4).

Datasets & Metrics Following Song et al. [2023c] and Chung et al. [2022a], we use the first 1000 image from LSUN Bedroom and LSUN Cat dataset [Yu et al., 2015] as test set. All images are resized into 256^2 . To evaluate sample quality, we use Fréchet Inception Distance [Heusel et al., 2017] and Kernel Inception Distance (KID) [Binkowski et al., 2018]. To evaluate consistency with the constraint, we use mIOU for segmentation and layout, CLIP score for captioning, and Accuracy for classification. For neural network $f(\cdot)$, we use different models for DIS and testing (See Appendix. B). For down-sampling, we use image restoration metrics such as LPIPS [Zhang et al., 2018] and peak signal-to-noise ratio (PSNR).

Previous State-of-the-Art DIS We compare our approach with previously published DIS that are able to solve neural network operator $f(\cdot)$. For methods that directly use posterior mean as posterior sample, we include DPS [Chung et al., 2022b], FreeDOM Yu et al. [2023] and MPGD [He et al., 2024]. For methods that construct an approximated posterior distribution with posterior mean as mode, we include LGD [Song et al., 2023b] and STSL [Rout et al., 2023] (See Tab. 2). We implement all those methods with EDM and Euler ancestral sampler (See details in Appendix. B). We acknowledge that there are other very competitive works designed for latent diffusion [Chung et al., 2023, Song et al., 2023a, He et al., 2023b, Rout et al., 2024] or linear operator $f(\cdot)$ [Meng and Kabashima, 2022, Dou and Song, 2023, Chung et al., 2022b, Song et al., 2022, Boys et al., 2023, He et al., 2023a]. However, for now we focus on pixel domain diffusion with neural network $f(\cdot)$, and have not included them for comparison.

4.2 Main Results

Results on Neural Network Operators We test our proposed approaches on four neural network operators: segmentation, layout estimation, caption and classification. As shown in Tab. 1, Fig. 1, Fig. 5, Fig. 10 and Fig. 11, both quantitatively and visually, our Proposed I (Sec. 3.4) has significant improvement on both consistency (*e.g.*, mIOU) and sample quality (*e.g.*, FID) over the baseline DPS [Chung et al., 2022a]. The advantage of our approximation over other posterior mean based approximations is clearly demonstrated. This is because neural network $f(\cdot)$ are sensitive to out-of-distribution input. On the other hand, our Proposed II (Sec. 3.5) is also quite effective compared with unconditional CM.

Results on Non-neural Network Operators In additional to neural network operators, we also verify that our approaches work well for non-neural network operators such as down-sampling. Results are summarized in Tab. 6 and Fig. 6. *lower*. Our Proposed I is only comparable to DPS for simple operators. This is because non-neural network $f(\cdot)$ are not that sensitive to out-of-distribution approximations. Besides, our Proposed II also works well for linear operator.

4.3 Ablation Study

We evaluate the effect of using CM for posterior approximation in Proposed I (Sec. 3.4) and adding randomness to CM in Proposed I & II (Sec. 3.4, Sec. 3.5) in Tab. 4. For Proposed I, we show that using CM to replace posterior mean reduces the distance with measurement y in mIOU and improves the sample quality in FID. Similarly, for both Proposed I & II, adding randomness improves mIOU and reduces FID.

Table 1: Results on neural network operators, *i.e.*, layout estimation, segmentation, caption and classification. **Bold**: best in diffusion-based DIS. Underline: second best in diffusion-based DIS.

	LSUN Bedroom						LSUN Cat					
	Segmentation			Layout			Caption			Classification		
	mIOU	FID	KID	mIOU	FID	KID	CLIP	FID	KID	Acc	FID	KID
<i>Diffusion Model based</i>												
EDM (Base)	0.17	6.35	1.4e-3	0.38	6.35	1.4e-3	21.27	6.35	1.4e-3	0.14	10.26	3.1e-3
DPS	0.27	22.84	1.0e-2	0.54	<u>7.59</u>	1.9e-3	22.57	9.49	2.6e-3	0.79	15.73	7.1e-3
FreeDOM	<u>0.27</u>	21.90	9.1e-3	0.46	15.27	8.1e-3	<u>22.61</u>	28.30	1.8e-2	<u>0.84</u>	32.32	1.7e-2
MPGD	0.24	82.66	6.9e-2	<u>0.73</u>	15.38	8.5e-3	21.49	21.14	1.3e-2	0.37	15.40	7.1e-3
LGD	0.22	35.69	2.4e-2	0.70	8.07	2.3e-3	22.58	<u>8.38</u>	<u>2.6e-3</u>	0.64	13.35	<u>4.5e-3</u>
STSL	<u>0.27</u>	19.48	7.4e-3	0.52	7.74	<u>2.2e-3</u>	22.39	9.70	2.8e-3	0.78	15.74	6.9e-3
Proposed I	0.34	18.06	<u>8.2e-3</u>	0.78	7.50	<u>2.2e-3</u>	22.63	8.16	2.5e-3	0.90	<u>13.45</u>	3.6e-3
<i>Consistency Model based</i>												
CM (Base)	0.18	20.45	1.0e-2	0.37	20.45	1.0e-2	21.40	20.45	1.0e-2	0.12	27.15	1.3e-2
Proposed II	0.32	32.60	2.2e-2	0.82	15.43	8.1e-3	22.56	14.86	6.7e-3	0.92	27.35	1.4e-2

Table 2: The posterior sample approximation of different methods.

	Approximation of posterior sample	Valid image?
DPS	$x_{0 t} = \mathbb{E}[X_0 X_t]$	✗
FreeDOM	$x_{0 t} = \mathbb{E}[X_0 X_t]$	✗
MDPG	$x_{0 t} = \mathbb{E}[X_0 X_t]$	✗
LGD	$x_{0 t} \sim \mathcal{N}(\mathbb{E}[X_0 X_t], r_t^2 I)$	✗
STSL	$x_{0 t} \sim \mathcal{N}(\mathbb{E}[X_0 X_t], \text{Cov}(X_0 X_t))$	✗
Proposed I	$x_{0 t} = g_\theta(t, X_t)$	✓

Table 3: Temporal and spatial complexity of different methods.

	Time (s)	VRAM (GB)
DPS	150	5.35
Proposed I	218	6.32
Proposed II	72	6.58

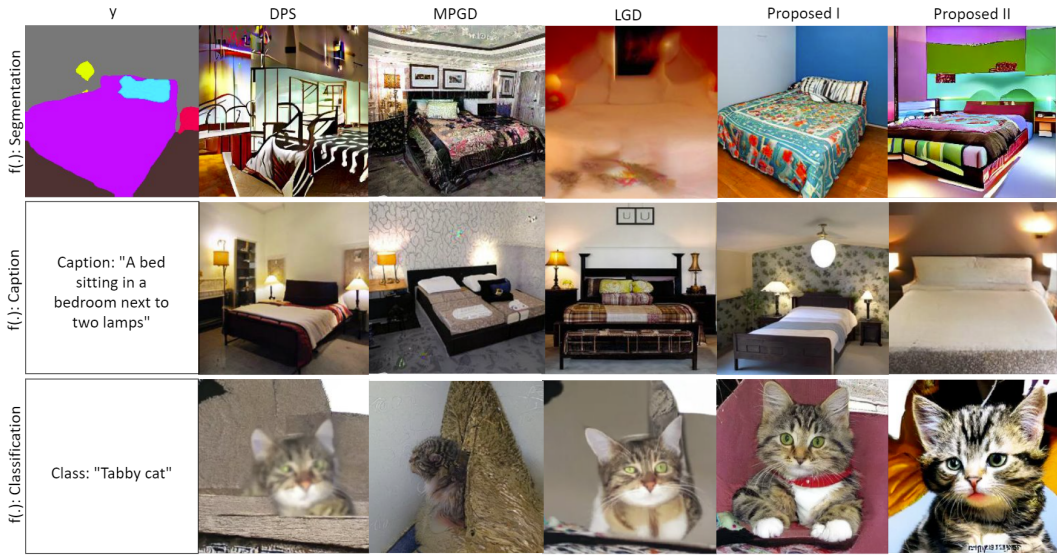


Figure 5: Visual results on neural network operators such as segmentation, caption and classification.

Table 4: Ablation study of Proposed I and Proposed II with Bedroom segmentation. **Bold**: Method with best performance.

	CM	Rand	mIOU	FID
Proposed I	✗	✗	0.27	22.84
	✓	✗	0.31	19.29
	✓	✓	0.34	18.06
Proposed II	-	✗	0.29	32.93
	-	✓	0.32	32.60

Table 5: Ablation study of randomness and data augmentation with segmentation.

Rand	mIOU		
	Model A	Model A + DA	Model B
✗	0.57	0.43	0.31
✓	0.51	0.54	0.34

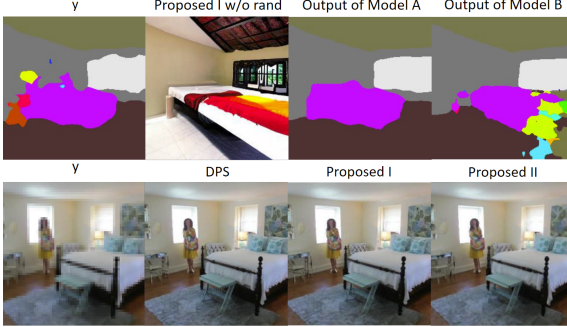


Figure 6: *upper*. An example of over-fitting an operator $f(\cdot)$. *lower*. Visual results on linear operators such as down-sampling.

Table 6: Results on non-neural network operators such as super-resolution.

	Bedroom Down-sampling (x4)			
	KID	FID	LPIPS	PSNR
<i>Diffusion Model based</i>				
EDM (Base)	1.4e-3	6.35	0.73	9.10
DPS	1.4e-3	<u>4.82</u>	0.11	26.69
FreeDOM	1.1e-3	4.84	0.11	<u>26.70</u>
MPGD	2.0e-3	43.36	0.38	22.84
LGD	2.8e-3	7.10	0.14	26.51
STSL	<u>1.2e-3</u>	4.80	<u>0.12</u>	26.65
Proposed I	1.9e-3	5.67	<u>0.12</u>	26.91
<i>Consistency Model based</i>				
CM (Base)	1.0e-2	20.45	0.73	9.49
Proposed II	2.9e-3	6.66	0.14	26.45

We assume that CM benefits from randomness as it avoids overfitting the operator $f(\cdot)$, or it makes $f(\cdot)$ robust to adversarial examples [Li et al., 2019]. To verify this assumption, we use Model A for $f(\cdot)$ during DIS. During testing $f(\cdot)$, we compare the results of Model A, Model A w/ data augmentation (DA), and a separate Model B. In Tab. 5, we show that when tested with Model A, the DIS w/o randomness outperform DIS w/ randomness. While on Model A w/ DA and Model B, the DIS w/ randomness outperforms DIS w/o randomness. This indicates that DIS w/o randomness overfits Model A. An example of such overfitting is presented in Fig. 6.*upper*.

4.4 Complexity

In Tab. 3, we show that Proposed I is 30% slower than DPS while Proposed II is 50% faster. Both of our approaches cost 1 GB more VRAM.

5 Related Work

Diffusion Inverse Solvers An important branch of DIS focus on linear operator $f(\cdot)$ with projection or pseudo-inverse [Wang et al., 2022, Kawar et al., 2022, Chung et al., 2022b, Lugmayr et al., 2022, Song et al., 2022, Dou and Song, 2023, Pokle et al., 2024, Cardoso et al., 2024]. For general, non-linear $f(\cdot)$, various approaches are proposed such as Monte carlo [Wu et al., 2024, Phillips et al., 2024], proximal gradient [Xu and Chi, 2024] and variational inference [Feng et al., 2023, Mardani et al., 2023, Janati et al., 2024]. Among those paradigms, the conditional score estimation methods are mostly adopted as they are scalable to practically large images with reasonable run-time [Chung et al., 2022a, Yu et al., 2023, Zhu et al., 2023, He et al., 2023c, Song et al., 2023b, Boys et al., 2023, Rout et al., 2023, 2024]. Following this paradigm, we propose to approximate posterior sample with PF-ODE, which improves the results for neural network $f(\cdot)$.

GAN Inverse Solvers Similar to diffusion inversion, given the measurement and operator, GAN inversion finds an image x on the prior of GAN by minimizing the distance of generated image and a target [Creswell and Bharath, 2016]. It is widely adopted for image editing and image restoration [Menon et al., 2020, Daras et al., 2021]. We propose to treat CM as several stacked GANs and invert CM as a series of GAN inversions.

6 Discussion & Conclusion

One major limitation of our work is that all the experiments are conducted with 256^2 images and diffusion models in pixel domain. Recent works already show the potential of CM on 512^2 for latent diffusion models [Luo et al., 2023, Chung et al., 2023, Song et al., 2023a, He et al., 2023b, Rout et al., 2024]. It would be interesting to see how our approach works empirically for large images using latent diffusion models.

To conclude, we show that the solution of PF-ODE is an effective posterior sample. Built upon this, we propose to use CM as a high-quality approximation to posterior sample. Further, we propose a new family of DIS using only CM. Experimental results show that our proposed approaches perform well for neural network operators.

References

- B. D. Anderson. Reverse-time diffusion equation models. *Stochastic Processes and their Applications*, 12(3):313–326, 1982.
- M. Binkowski, D. J. Sutherland, M. Arbel, and A. Gretton. Demystifying mmd gans. *ArXiv*, abs/1801.01401, 2018. URL <https://api.semanticscholar.org/CorpusID:3531856>.
- Y. Blau and T. Michaeli. The perception-distortion tradeoff. In *Proceedings of the IEEE conference on computer vision and pattern recognition*, pages 6228–6237, 2018.
- B. Boys, M. Girolami, J. Pidstrigach, S. Reich, A. Mosca, and O. D. Akyildiz. Tweedie moment projected diffusions for inverse problems. *arXiv preprint arXiv:2310.06721*, 2023.
- G. Cardoso, Y. J. el idrissi, S. L. Corff, and E. Moulines. Monte carlo guided denoising diffusion models for bayesian linear inverse problems. In *The Twelfth International Conference on Learning Representations*, 2024. URL <https://openreview.net/forum?id=nHESwXvxwK>.
- H. Chung, J. Kim, M. T. McCann, M. L. Klasky, and J. C. Ye. Diffusion posterior sampling for general noisy inverse problems. *ArXiv*, abs/2209.14687, 2022a. URL <https://api.semanticscholar.org/CorpusID:252596252>.
- H. Chung, B. Sim, D. Ryu, and J. C. Ye. Improving diffusion models for inverse problems using manifold constraints. *ArXiv*, abs/2206.00941, 2022b. URL <https://api.semanticscholar.org/CorpusID:249282628>.
- H. Chung, J. C. Ye, P. Milanfar, and M. Delbracio. Prompt-tuning latent diffusion models for inverse problems. *ArXiv*, abs/2310.01110, 2023. URL <https://api.semanticscholar.org/CorpusID:263605744>.
- A. Creswell and A. A. Bharath. Inverting the generator of a generative adversarial network. *IEEE Transactions on Neural Networks and Learning Systems*, 30:1967–1974, 2016. URL <https://api.semanticscholar.org/CorpusID:3621348>.
- G. Daras, J. Dean, A. Jalal, and A. G. Dimakis. Intermediate layer optimization for inverse problems using deep generative models. In *International Conference on Machine Learning*, 2021. URL <https://api.semanticscholar.org/CorpusID:231925054>.
- Z. Dou and Y. Song. Diffusion posterior sampling for linear inverse problem solving: A filtering perspective. In *The Twelfth International Conference on Learning Representations*, 2023.
- B. Efron. Tweedie’s formula and selection bias. *Journal of the American Statistical Association*, 106:1602–1614, 2011. URL <https://api.semanticscholar.org/CorpusID:23284154>.
- B. T. Feng, J. Smith, M. Rubinstein, H. Chang, K. L. Bouman, and W. T. Freeman. Score-based diffusion models as principled priors for inverse imaging. *arXiv preprint arXiv:2304.11751*, 2023.
- K. He, X. Zhang, S. Ren, and J. Sun. Deep residual learning for image recognition. *2016 IEEE Conference on Computer Vision and Pattern Recognition (CVPR)*, pages 770–778, 2015. URL <https://api.semanticscholar.org/CorpusID:206594692>.
- L. He, H. Yan, M. Luo, K. Luo, W. Wang, W. Du, H. Chen, H. ling Yang, and Y. Zhang. Fast and stable diffusion inverse solver with history gradient update. 2023a. URL <https://api.semanticscholar.org/CorpusID:260124974>.
- L. He, H. Yan, M. Luo, K. Luo, W. Wang, W. Du, H. Chen, H. Yang, and Y. Zhang. Iterative reconstruction based on latent diffusion model for sparse data reconstruction. *ArXiv*, abs/2307.12070, 2023b. URL <https://api.semanticscholar.org/CorpusID:268678282>.

- Y. He, N. Murata, C.-H. Lai, Y. Takida, T. Uesaka, D. Kim, W.-H. Liao, Y. Mitsufuji, J. Z. Kolter, R. Salakhutdinov, and S. Ermon. Manifold preserving guided diffusion. *ArXiv*, abs/2311.16424, 2023c. URL <https://api.semanticscholar.org/CorpusID:265466093>.
- Y. He, N. Murata, C.-H. Lai, Y. Takida, T. Uesaka, D. Kim, W.-H. Liao, Y. Mitsufuji, J. Z. Kolter, R. Salakhutdinov, et al. Manifold preserving guided diffusion. In *The Twelfth International Conference on Learning Representations*, 2024. URL <https://openreview.net/forum?id=o3Bx0Loxm1>.
- J. Hessel, A. Holtzman, M. Forbes, R. L. Bras, and Y. Choi. Clipscore: A reference-free evaluation metric for image captioning. *ArXiv*, abs/2104.08718, 2021. URL <https://api.semanticscholar.org/CorpusID:233296711>.
- M. Heusel, H. Ramsauer, T. Unterthiner, B. Nessler, and S. Hochreiter. Gans trained by a two time-scale update rule converge to a local nash equilibrium. In *Neural Information Processing Systems*, 2017. URL <https://api.semanticscholar.org/CorpusID:326772>.
- J. Ho, A. Jain, and P. Abbeel. Denoising diffusion probabilistic models. *Advances in neural information processing systems*, 33:6840–6851, 2020.
- Y. Janati, A. Durmus, E. Moulines, and J. Olsson. Divide-and-conquer posterior sampling for denoising diffusion priors. *arXiv preprint arXiv:2403.11407*, 2024.
- T. Karras, M. Aittala, T. Aila, and S. Laine. Elucidating the design space of diffusion-based generative models. *ArXiv*, abs/2206.00364, 2022. URL <https://api.semanticscholar.org/CorpusID:249240415>.
- B. Kawar, M. Elad, S. Ermon, and J. Song. Denoising diffusion restoration models. *ArXiv*, abs/2201.11793, 2022. URL <https://api.semanticscholar.org/CorpusID:246411364>.
- D. P. Kingma, T. Salimans, B. Poole, and J. Ho. Variational diffusion models. *ArXiv*, abs/2107.00630, 2021. URL <https://api.semanticscholar.org/CorpusID:235694314>.
- C. Ledig, L. Theis, F. Huszár, J. Caballero, A. Cunningham, A. Acosta, A. Aitken, A. Tejani, J. Totz, Z. Wang, et al. Photo-realistic single image super-resolution using a generative adversarial network. In *Proceedings of the IEEE conference on computer vision and pattern recognition*, pages 4681–4690, 2017.
- B. Li, C. Chen, W. Wang, and L. Carin. Certified adversarial robustness with additive noise. *Advances in neural information processing systems*, 32, 2019.
- J. Li, D. Li, C. Xiong, and S. Hoi. Blip: Bootstrapping language-image pre-training for unified vision-language understanding and generation. In *ICML*, 2022.
- X. Li, Y. Ren, X. Jin, C. Lan, X. Wang, W. Zeng, X. Wang, and Z. Chen. Diffusion models for image restoration and enhancement—a comprehensive survey. *arXiv preprint arXiv:2308.09388*, 2023.
- H.-J. Lin, S.-W. Huang, S.-H. Lai, and C.-K. Chiang. Indoor scene layout estimation from a single image. *2018 24th International Conference on Pattern Recognition (ICPR)*, pages 842–847, 2018. URL <https://api.semanticscholar.org/CorpusID:54212984>.
- A. Lugmayr, M. Danelljan, A. Romero, F. Yu, R. Timofte, and L. V. Gool. Repaint: Inpainting using denoising diffusion probabilistic models. *2022 IEEE/CVF Conference on Computer Vision and Pattern Recognition (CVPR)*, pages 11451–11461, 2022. URL <https://api.semanticscholar.org/CorpusID:246240274>.
- S. Luo, Y. Tan, L. Huang, J. Li, and H. Zhao. Latent consistency models: Synthesizing high-resolution images with few-step inference. *ArXiv*, abs/2310.04378, 2023. URL <https://api.semanticscholar.org/CorpusID:263831037>.
- M. Mardani, J. Song, J. Kautz, and A. Vahdat. A variational perspective on solving inverse problems with diffusion models. *ArXiv*, abs/2305.04391, 2023. URL <https://api.semanticscholar.org/CorpusID:258557287>.

- X. Meng and Y. Kabashima. Diffusion model based posterior sampling for noisy linear inverse problems. *ArXiv*, abs/2211.12343, 2022. URL <https://api.semanticscholar.org/CorpusID:253761055>.
- S. Menon, A. Damian, S. Hu, N. Ravi, and C. Rudin. Pulse: Self-supervised photo upsampling via latent space exploration of generative models. *2020 IEEE/CVF Conference on Computer Vision and Pattern Recognition (CVPR)*, pages 2434–2442, 2020. URL <https://api.semanticscholar.org/CorpusID:212634162>.
- B. B. Moser, A. S. Shanbhag, F. Raue, S. Frolov, S. Palacio, and A. Dengel. Diffusion models, image super-resolution and everything: A survey. *arXiv preprint arXiv:2401.00736*, 2024.
- A. Phillips, H.-D. Dau, M. J. Hutchinson, V. D. Bortoli, G. Deligiannidis, and A. Doucet. Particle denoising diffusion sampler. *ArXiv*, abs/2402.06320, 2024. URL <https://api.semanticscholar.org/CorpusID:267616914>.
- A. Pokle, M. J. Muckley, R. T. Q. Chen, and B. Karrer. Training-free linear image inversion via flows, 2024. URL <https://openreview.net/forum?id=3JoQqW35GQ>.
- L. Rout, Y. Chen, A. Kumar, C. Caramanis, S. Shakkottai, and W.-S. Chu. Beyond first-order tweedie: Solving inverse problems using latent diffusion. *ArXiv*, abs/2312.00852, 2023. URL <https://api.semanticscholar.org/CorpusID:265609906>.
- L. Rout, N. Raoof, G. Daras, C. Caramanis, A. Dimakis, and S. Shakkottai. Solving linear inverse problems provably via posterior sampling with latent diffusion models. *Advances in Neural Information Processing Systems*, 36, 2024.
- J. Sohl-Dickstein, E. Weiss, N. Maheswaranathan, and S. Ganguli. Deep unsupervised learning using nonequilibrium thermodynamics. In *International conference on machine learning*, pages 2256–2265. PMLR, 2015.
- B. Song, S. M. Kwon, Z. Zhang, X. Hu, Q. Qu, and L. Shen. Solving inverse problems with latent diffusion models via hard data consistency. *arXiv preprint arXiv:2307.08123*, 2023a.
- J. Song, A. Vahdat, M. Mardani, and J. Kautz. Pseudoinverse-guided diffusion models for inverse problems. In *International Conference on Learning Representations*, 2022.
- J. Song, Q. Zhang, H. Yin, M. Mardani, M.-Y. Liu, J. Kautz, Y. Chen, and A. Vahdat. Loss-guided diffusion models for plug-and-play controllable generation. In *International Conference on Machine Learning*, 2023b. URL <https://api.semanticscholar.org/CorpusID:260957043>.
- Y. Song, J. Sohl-Dickstein, D. P. Kingma, A. Kumar, S. Ermon, and B. Poole. Score-based generative modeling through stochastic differential equations. *arXiv preprint arXiv:2011.13456*, 2020.
- Y. Song, P. Dhariwal, M. Chen, and I. Sutskever. Consistency models. In *International Conference on Machine Learning*, 2023c. URL <https://api.semanticscholar.org/CorpusID:257280191>.
- C. Szegedy, W. Zaremba, I. Sutskever, J. Bruna, D. Erhan, I. Goodfellow, and R. Fergus. Intriguing properties of neural networks. *arXiv preprint arXiv:1312.6199*, 2013.
- R. Vershynin. *High-dimensional probability: An introduction with applications in data science*, volume 47. Cambridge university press, 2018.
- Y. Wang, J. Yu, and J. Zhang. Zero-shot image restoration using denoising diffusion null-space model. *ArXiv*, abs/2212.00490, 2022. URL <https://api.semanticscholar.org/CorpusID:254125609>.
- L. Wu, B. Trippe, C. Naesseth, D. Blei, and J. P. Cunningham. Practical and asymptotically exact conditional sampling in diffusion models. *Advances in Neural Information Processing Systems*, 36, 2024.
- X. Xu and Y. Chi. Provably robust score-based diffusion posterior sampling for plug-and-play image reconstruction. *arXiv preprint arXiv:2403.17042*, 2024.

- F. Yu, Y. Zhang, S. Song, A. Seff, and J. Xiao. Lsun: Construction of a large-scale image dataset using deep learning with humans in the loop. *arXiv preprint arXiv:1506.03365*, 2015.
- J. Yu, Y. Wang, C. Zhao, B. Ghanem, and J. Zhang. Freedom: Training-free energy-guided conditional diffusion model. *ArXiv*, abs/2303.09833, 2023. URL <https://api.semanticscholar.org/CorpusID:257622962>.
- R. Zhang, P. Isola, A. A. Efros, E. Shechtman, and O. Wang. The unreasonable effectiveness of deep features as a perceptual metric. *2018 IEEE/CVF Conference on Computer Vision and Pattern Recognition*, pages 586–595, 2018. URL <https://api.semanticscholar.org/CorpusID:4766599>.
- B. Zhou, H. Zhao, X. Puig, S. Fidler, A. Barriuso, and A. Torralba. Scene parsing through ade20k dataset. In *Proceedings of the IEEE Conference on Computer Vision and Pattern Recognition*, 2017.
- Y. Zhu, K. Zhang, J. Liang, J. Cao, B. Wen, R. Timofte, and L. Van Gool. Denoising diffusion models for plug-and-play image restoration. In *Proceedings of the IEEE/CVF Conference on Computer Vision and Pattern Recognition (CVPR) Workshops*, pages 1219–1229, June 2023.

A Proof of Main Results

We first derive some basic properties of the GMM model. More specifically, we have

$$p_\theta(X_0) = \frac{1}{N} \sum_{i=1}^N \mathcal{N}(X_0|\mu^i, \sigma^2 I), \quad (14)$$

$$p_\theta(X_t|X_0) = \mathcal{N}(X_t|X_0, \sigma_t^2 I), \quad (15)$$

$$p_\theta(X_t) = \frac{1}{N} \sum_{i=1}^N \mathcal{N}(X_t|\mu^i, (\sigma^2 + \sigma_t^2)I), \quad (16)$$

$$\begin{aligned} p_\theta(X_0|X_t) &= \frac{p_\theta(X_t|X_0)p_\theta(X_0)}{p_\theta(X_t)} \\ &= \sum_{i=1}^N \frac{\mathcal{N}(X_t|X_0)}{\sum_{j=1}^N \mathcal{N}(X_t|\mu^j, (\sigma^2 + \sigma_t^2)I)} \mathcal{N}(X_0|\mu^i, \sigma^2 I) \\ &= \sum_{i=1}^N u_i \mathcal{N}(X_0|\mu^i, \sigma^2 I), \end{aligned}$$

$$\text{where } u_i = (\exp - \frac{\|X_0 - X_t\|^2}{2\sigma_t^2}) / (\sum_{j=1}^N \frac{1}{\sqrt{(1 + \sigma^2/\sigma_t^2)^d}} \exp - \frac{\|X_t - \mu^j\|^2}{2(\sigma^2 + \sigma_t^2)}). \quad (17)$$

For true posterior $p_\theta(X_0|X_t = x_t)$, we know that X_0 eventually converges to one of the μ^i . Therefore, the μ^* closest to X_t will have highest weighting u_i . And thus no matter what is the value of σ_t^2 , the highest density mode of true posterior is always the mode μ^* that is closest to the initial point x_t . And the decision boundary is always the voronoi centered at μ^i .

Lemma 3.3 *The PF-ODE can be written as:*

$$\frac{dX_t}{dt} = \underbrace{\sum_{i=1}^N \frac{w_i}{2} \frac{d\sigma_t^2}{dt} \frac{(X_t - \mu^i)}{\sigma^2 + \sigma_t^2}}_{\text{velocity field } v_t}, w_i = (\exp - \frac{\|X_t - \mu^i\|^2}{2(\sigma^2 + \sigma_t^2)}) / (\sum_{j=1}^N \exp - \frac{\|X_t - \mu^j\|^2}{2(\sigma^2 + \sigma_t^2)}).$$

Proof. We need to compute the score function first:

$$\begin{aligned} \nabla \log p_\theta(X_t = x_t) &= \frac{\nabla p_\theta(X_t = x_t)}{p_\theta(X_t = x_t)} \\ &= \frac{1}{p_\theta(X_t = x_t)} \nabla \left(\sum_{i=1}^N \frac{1}{N} (\mathcal{N}(X_t = x_t|\mu^i, (\sigma^2 + \sigma_t^2)I)) \right) \\ &= \frac{1}{p_\theta(X_t = x_t)} \sum_{i=1}^N \frac{1}{N} \mathcal{N}(X_t = x_t|\mu^i, (\sigma^2 + \sigma_t^2)) \left(-\frac{(x - \mu^i)}{\sigma^2 + \sigma_t^2} \right) \\ &= \sum_{i=1}^N \left((\exp - \frac{\|x_t - \mu^i\|^2}{2(\sigma^2 + \sigma_t^2)}) / (\sum_{j=1}^N \exp - \frac{\|x_t - \mu^j\|^2}{2(\sigma^2 + \sigma_t^2)}) \right) \left(-\frac{x - \mu^i}{\sigma^2 + \sigma_t^2} \right). \end{aligned} \quad (18)$$

Take the score function into the PF-ODE definition in Eq. 3, we can obtain the result. \square

With those basic properties, we can show that the solution of PF-ODE with initial value $X_t = x_t$ has non-zero density in true posterior $p_\theta(X_0|X_t)$.

Proposition 3.2 *The solution of PF-ODE has a positive likelihood in true posterior with high probability, i.e.,*

$$p_\theta(X_0 = \Phi(x_t)|X_t = x_t) \geq \frac{1}{N} \frac{1}{\sqrt{(4\pi\sigma^2)^d}} \exp(-\frac{2c^2}{\sigma_t^2} - \frac{d+1}{2}), \text{ with probability } 1 - p. \quad (19)$$

Proof.

$$p_\theta(X_0 = \Phi(x_t)|X_t = x_t) = \sum_{i=1}^N u_i \mathcal{N}(X_0 = \Phi(x_t)|\mu^i, \sigma^2 I) \quad (20)$$

$$\geq u_j \mathcal{N}(X_0 = \Phi(x_t)|\mu^j, \sigma^2 I), \forall j \quad (21)$$

We let $k = \min_i \{|\mu^i - \Phi(x_t)|\}$, by assumption we have $\|\Phi_0(x_t) - \mu^k\| \leq \sigma^2 + d\sigma^2$ with probability $1 - p$.

$$p_\theta(X_0 = \Phi(x_t)|X_t = x_t) \geq u_k \frac{1}{\sqrt{(2\pi\sigma^2)^d}} \exp - \frac{\|\mu^k - \Phi(x_t)\|^2}{2\sigma^2} \quad (22)$$

$$\stackrel{(a)}{\geq} u_k \frac{1}{\sqrt{(2\pi\sigma^2)^d}} \exp - \frac{(d+1)\sigma^2}{2\sigma^2} \quad (23)$$

$$= \frac{\exp - \frac{\|\Phi(x_t) - x_t\|^2}{2\sigma_t^2}}{\sum_{j=1}^N \sqrt{(1 + \sigma^2/\sigma_t^2)^d} \exp - \frac{\|x_t - \mu^j\|^2}{2(\sigma^2 + \sigma_t^2)}} \frac{1}{\sqrt{(2\pi\sigma^2)^d}} \exp - \frac{d+1}{2} \quad (24)$$

$$\stackrel{(b)}{\geq} \frac{\exp - \frac{4c^2}{2\sigma_t^2}}{\sqrt{2^d} \sum_{j=1}^N \exp 0} \frac{1}{\sqrt{(2\pi\sigma^2)^d}} \exp - \frac{d+1}{2} \quad (25)$$

$$= \frac{1}{N} \frac{1}{\sqrt{(4\pi\sigma^2)^d}} \exp \left(-\frac{2c^2}{\sigma_t^2} - \frac{d+1}{2} \right) \quad (26)$$

(a) is due to the assumption that $\|\Phi(x_t) - \mu^k\|^2 \leq \sigma^2 + d\sigma^2$. (b) is due to $\|\Phi_0(x_t) - x_t\| \leq \|\Phi_0(x_t)\| + \|x_t\|$. As they are both bounded by c , $\|\Phi_0(x_t) - x_t\|^2$ is bounded by $4c^2$. And $1 + \frac{\sigma^2}{\sigma_t^2} \leq 2$. \square

We can study the PF-ODE in Eq. 11 informally when σ_t^2 is rather small or large. When σ_t^2 is small, the soft-max w_i becomes a "hard"-max. Denote $k = \min_i \{|\mu^i - \Phi(x_t)|\}$ and the PF-ODE at that time can be written as

$$\frac{dX_t}{dt} = -\frac{1}{2} \frac{d\sigma_t^2}{dt} \left(-\frac{(X_t - \mu^k)}{\sigma^2 + \sigma_t^2} \right). \quad (27)$$

At that time, the PF-ODE is first order separable. And we can solve it with initial value $X_t = x_t$ as

$$\frac{\Phi(x_t) - \mu^k}{x_t - \mu^k} = e^{h(t)}, \quad (28)$$

where $h(\cdot)$ is some function of t related to the $d\sigma_t^2/dt$.

Let's assume a simple σ_t^2 schedule such as $\sigma_t^2 = t^2$. In that case, we have

$$\Phi(x_t) = \mu^k + (x_t - \mu^k) e^{\frac{1}{2} \ln \frac{\sigma^2}{\sigma^2 + t^2}}. \quad (29)$$

The solution has the form of μ^k with an offset term weighted by an exponential term. When σ^2 is small, the exponential term goes to 0 very fast. And therefore $\Phi(x_t) \approx \mu^k$ at that time.

B Additional Experiment Setup

B.1 Implementation Details

All the experiments are implemented in Pytorch, and run in a computer with AMD EPYC 7742 CPU and Nvidia A100 GPU.

As we have shown, using the same model for $f(\cdot)$ causes overfitting for neural network based $f(\cdot)$. Therefore, we adopt different model for $f(\cdot)$ in DIS and testing, and the details are shown in Tab. 7.

For different operators, we also have different $d(\cdot, \cdot)$ to evaluate the distance $d(f(x_{0|t}), y)$ during the DIS process. For all four non-linear operators, the cross entropy are used for $d(\cdot, \cdot)$. While for

Table 7: The model specification used for different non-linear operators.

	Model A	Model B
Segmentation	MobileNet + C1	ResNet50 + PPM
Layout	Lin et al. [2018]	Lin et al. [2018] + DA
Caption	BLIP	CLIP
Classification	ResNet50	VITB16

Table 8: Metrics for DIS loss and evaluation.

	$d(., .)$ for DIS	metric for Test
Segmentation	Cross Entropy	mIOU
Layout	Cross Entropy	mIOU
Caption	Cross Entropy	CLIP score
Classification	Cross Entropy	Accuracy
Downsample	MSE	MSE

down-sample, we adopt MSE. To evaluate how consistent the generated samples are to y , we use y-metrics. Or to say, the metrics computed with input measurement y and $f(x_{0|t})$. More specifically, for Segmentation and Layout, we evaluate consistency by y-mIOU. For image caption, we evaluate consistency by CLIP score [Hessel et al., 2021]. For classification, we evaluate consistency by accuracy. And for down-sample, we evaluate consistency by MSE. Note that the $d(., .)$ used during DIS follows the convention of training corresponding $f(., .)$, and the y-metric used for testing also follows the convention of testing corresponding $f(., .)$.

B.2 Details of DIS Algorithm

Below we provide detailed algorithm of different DIS methods including the ones we compare to and our own.

Algorithm 1: DPS

```

1 procedure
  DPS( $p_\theta(\cdot|\cdot), T, f(\cdot), y, d(\cdot, \cdot), \zeta_t$ )
2    $x_T = \mathcal{N}(0, T^2 I)$ 
3   for  $t = T$  to 1 do
4      $x_{t-1} \sim p_\theta(X_{t-1}|X_t = x_t)$ 
5      $x_{0|t} = \mathbb{E}[X_0|X_t = x_t]$ 
6      $x_{t-1} \leftarrow x_{t-1} - \zeta_t d(f(x_{0|t}), y)$ 
7   return  $x_0$ 

```

Algorithm 2: FreeDOM

```

1 procedure
  FreeDOM( $p_\theta(\cdot|\cdot), q(\cdot|\cdot), T, f(\cdot), y, d(\cdot, \cdot), \zeta_t, r, K$ )
2    $x_T = \mathcal{N}(0, T^2 I)$ 
3   for  $t = T$  to 1 do
4     for  $t' = K$  to 1 do
5        $x_{t-1} \sim p_\theta(X_{t-1}|X_t = x_t)$ 
6        $x_{0|t} = \mathbb{E}[X_0|X_t = x_t]$ 
7        $x_{t-1} \leftarrow x_{t-1} - \zeta_t d(f(x_{0|t}), y)$ 
8       if  $t' \neq 1, t \in r$  then
9          $x_t = q(X_t|X_{t-1} = x_{t-1})$ 
10      else
11        break
12   return  $x_0$ 

```

Algorithm 3: MPGD

```

1 procedure
  MPGD( $q_\theta(\cdot|\cdot), T, f(\cdot), y, d(\cdot, \cdot), \zeta_t$ )
2    $x_T = \mathcal{N}(0, T^2 I)$ 
3   for  $t = T$  to 1 do
4      $x_{0|t} = \mathbb{E}[X_0|X_t = x_t]$ 
5      $x_{0|t} \leftarrow x_{0|t} - \zeta_t d(f(x_{0|t}), y)$ 
6      $x_{t-1} \leftarrow q(X_{t-1}|X_t = x_t, X_t = x_{0|t})$ 
7   return  $x_0$ 

```

Algorithm 4: LGD (Single Sample)

```

1 procedure
  LGD( $p_\theta(\cdot|\cdot), T, f(\cdot), y, d(\cdot, \cdot), \zeta_t, r_t$ )
2    $x_T = \mathcal{N}(0, T^2 I)$ 
3   for  $t = T$  to 1 do
4      $x_{t-1} \sim p_\theta(X_{t-1}|X_t = x_t)$ 
5      $x_{0|t} = \mathbb{E}[X_0|X_t = x_t] + \mathcal{N}(0, r_t^2 I)$ 
6      $x_{t-1} \leftarrow x_{t-1} - \zeta_t d(f(x_{0|t}), y)$ 
7   return  $x_0$ 

```

Algorithm 5: STSL (Single Sample)

```

1 procedure
  STSL( $p_\theta(\cdot|\cdot), T, f(\cdot), y, d(\cdot, \cdot), \zeta_t, \eta_t$ )
2    $x_T = \mathcal{N}(0, T^2 I)$ 
3   for  $t = T$  to 1 do
4      $x_{0|t} = \mathbb{E}[X_0|X_t = x_t]$ 
5      $x_t \leftarrow x_t - \zeta_t d(f(x_{0|t}), y)$ 
6      $\epsilon \sim \mathcal{N}(0, I)$ 
7      $x_t \leftarrow$ 
       $x_t - \eta_t \nabla_{x_t} (\epsilon^T (s_\theta(t, x_t + \epsilon) - s_\theta(t, x_t)))$ 
8      $x_{t-1} \sim p_\theta(X_{t-1}|X_t = x_t)$ 
9   return  $x_0$ 

```

Algorithm 6: Proposed I

```

1 procedure Proposed-
  I( $p_\theta(\cdot|\cdot), T, f(\cdot), y, d(\cdot, \cdot), \zeta_t, g_\theta(\cdot, \cdot), \tau$ )
2    $x_T = \mathcal{N}(0, T^2 I)$ 
3   for  $t = T$  to 1 do
4      $x_{t-1} \sim p_\theta(X_t|X_{t-1} = x_{t-1})$ 
5      $x_{0|t} = g_\theta(t, x_t) + \mathcal{N}(0, \tau^2 I)$ 
6      $x_{t-1} \leftarrow x_{t-1} - \zeta_t d(f(x_{0|t}), y)$ 
7   return  $x_0$ 

```

Algorithm 7: Consistency Model

```

1 procedure CM( $g_\theta(\cdot, \cdot), t_{1:N}$ )
2   for  $n = 1$  to  $N - 1$  do
3      $z \sim \mathcal{N}(0, I)$ 
4      $x_{t_n} \leftarrow x_0 + t_n z$ 
5      $x_0 \leftarrow g_\theta(t_n, x_{t_n})$ 
6   return  $x_0$ 

```

Algorithm 8: Proposed II

```

1 procedure CMInversion( $g_\theta(\cdot, \cdot), t_{1:N}, f(\cdot),$ 
   $y, \tau$ )
2   for  $n = 1$  to  $N - 1$  do
3      $z \sim \mathcal{N}(0, I)$ 
4     for  $k = 1$  to  $K$  do
5        $x_{t_n} \leftarrow x_0 + t_n z$ 
6        $x_0 \leftarrow g_\theta(t_n, x_{t_n})$ 
7        $x_\tau \leftarrow x_0 + \mathcal{N}(0, \tau^2 I)$ 
8        $z \leftarrow z - \zeta \frac{d}{dz} d(f(x_\tau), y)$ 
9   return  $x_0$ 

```

FreeDOM Yu et al. [2023] propose to adopt the time-travel that is designed specifically for inpainting [Lugmayr et al., 2022] to general operator $f(\cdot)$. (See Algorithm. 2) More specifically, it proposes an inner loop that goes forward after a backward step with forward kernel $q(\cdot|\cdot)$. The new hyper-parameters are time-travel steps K and time-travel range r .

MPGD He et al. [2023c] propose to perform the gradient ascent directly on posterior mean instead of on x_t . And the posterior mean after gradient ascent is used to correct the score function (See Algorithm. 3). They claim that their approach is able to converge faster and outperform DPS when $T = 20, 100$. However, as we use $T = 1000$, the advantage of their approach is not clearly shown in our experiments.

LGD Song et al. [2023b] adopt a Gaussian approximation to posterior sample (See Algorithm. 4). More specifically, they use an additive of Gaussian noise and posterior mean as an approximation of Gaussian sample. And the mean of approximated sample is the same as real posterior sample. This approach is later improved by Boys et al. [2023], Rout et al. [2023] to second order. Or to say, they estimate the covariance of Gaussian using second order Tweedie’s formula. And the mean and covariance of approximated sample is the same as real posterior sample. The authors of LGD further propose a multi-sample approach to reduce gradient variance. However, we only use LGD with sample size $n = 1$ for fair comparison. The new hyper-parameters is variance τ .

STSL Rout et al. [2023] propose to improve Song et al. [2023b] by estimating the posterior as Gaussian distribution with posterior mean and posterior covariance. As directly estimating the

posterior covariance using second order Tweedie’s formula is expensive, they propose a Monte Carlo estimation and the resulting algorithm is shown in Algorithm. 5. However, we only use STSL with sample size $n = 1$ for fair comparison.

B.3 Hyper-parameters

	Segmentation	Layout	Caption	Classification	Down-sampling
DPS	$\zeta = 256.0$	$\zeta = 7.2$	$\zeta = 24.0$	$\zeta = 8.0$	$\zeta = 14.4$
LGD	$\zeta = 256.0$	$\zeta = 7.2$	$\zeta = 24.0$ $K = 1, \tau = 0.2$	$\zeta = 8.0$	$\zeta = 14.4$
FreeDOM	$\zeta = 256.0$	$\zeta = 7.2$	$\zeta = 24.0$ $K = 2, r = [100, 200]$	$\zeta = 8.0$	$\zeta = 14.4$
MPGD	$\zeta = 2560.0$	$\zeta = 72.0$	$\zeta = 240.0$	$\zeta = 80.0$	$\zeta = 144.0$
Proposed I	$\zeta = 256.0$	$\zeta = 7.2$	$\zeta = 24.0$ $\tau = 0.2$	$\zeta = 8.0$	$\zeta = 14.4$
Proposed II	$\zeta_1 = 0.1, \zeta_2 = 0.005$ $ts = 3, 6, \dots, 18, 30, 39$ $K = 40$	$\zeta_1 = 0.1, \zeta_2 = 0.001$ $ts = 75, 100, 125, 150$ $K = 151$	$\zeta_1 = 0.1, \zeta_2 = 0.001$ $ts = 75, 100, 125, 150$ $K = 151$	$\zeta_1 = 0.1, \zeta_2 = 0.005$ $ts = 25, 50, 75, 125, 150$ $K = 151$	$\zeta_1 = 0.3, \zeta_2 = 0.03$ $ts = 75, 100, 125, 150$ $K = 151$

Table 9: The hyper-parameters of other DIS and proposed approaches.

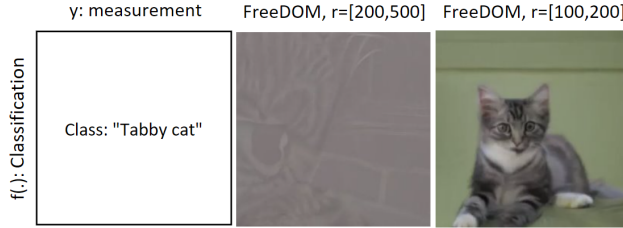


Figure 7: Comparison of different inner-loop range for FreeDOM.

We list the detailed hyper-parameters of DPS, LGD, FreeDOM, MPGD [Chung et al., 2022a, Song et al., 2023b, Yu et al., 2023, He et al., 2024] and two of our proposed approaches in Tab. 9. For all the methods, one common hyper-parameter is the step size ζ used in gradient descent. For LGD and our Proposed I, an additional hyper-parameter is the additional additive noise $\tau = 0.2$. We do not use the multi-sample LGD as it is significantly slower than all other approaches. For FreeDOM, the additional parameters are time-travel steps K , and time-travel range r . We set $K = 2$ for fair comparison, as a large K make FreeDOM significantly slower than all other approaches. We set $r = [100, 200]$ instead of $r = [200, 500]$ in original paper [Yu et al., 2023]. This is because we find that setting $r = [200, 500]$ in VE-diffusion has significant negative effect on sample quality. The visual comparison is in Fig. 7. For Proposed II, in addition to learning rate ζ , we also control the timestep schedule ts and optimization step K .

C Additional Experiment Results

C.1 Additional Visual Results

We present more visual results of non-linear operators in Fig. 10 and 11. It is shown that our Proposed I has best consistency with measurement y and best sample quality for most of the times. Our Proposed II also has a good consistency and sample quality.

Furthermore, we present more visual results of down-sampling in Fig. 8. It is shown that both our Proposed II and Proposed II work as good as DPS.

C.2 Failure Cases

When the measurement y is too far from diffusion prior, our approaches and other DIS approaches fail. An example of such failure is shown in Fig. 9. The input measurement y describes a woman. However, human is not a part of LSUN bedroom dataset. And none-of the DIS approaches is able to generate a woman. And the samples generated by DIS look like unconditional sample.

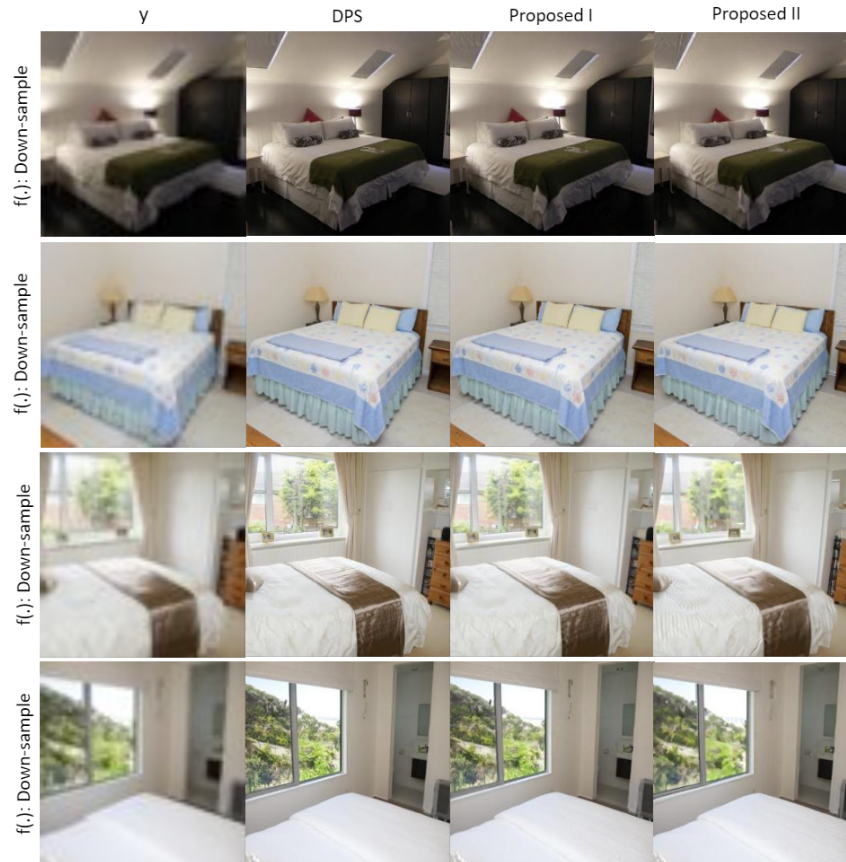


Figure 8: Additional visual results on image down-sampling.

D Additional Discussion

D.1 Reproducibility Statement

The proof of all theoretical results are shown in Appendix. A. For experiments, all two datasets are publicly available. In Appendix. B, we provide additional implementation details of all other DIS that we compare to. Further, detailed hyper-parameters of all baselines and our proposed approach are presented. Besides, we provide source code for reproducing empirical results as supplementary material.

D.2 Broader Impact

The approach proposed in this paper allows conditional generation without training a new model. This saves the energy of training conditional generative diffusion model and reduces the carbon emission. Potential negative impact is the same as other conditional generative model, such as trustworthiness brought by generating fake image.



Figure 9: Visual results of a failure case.

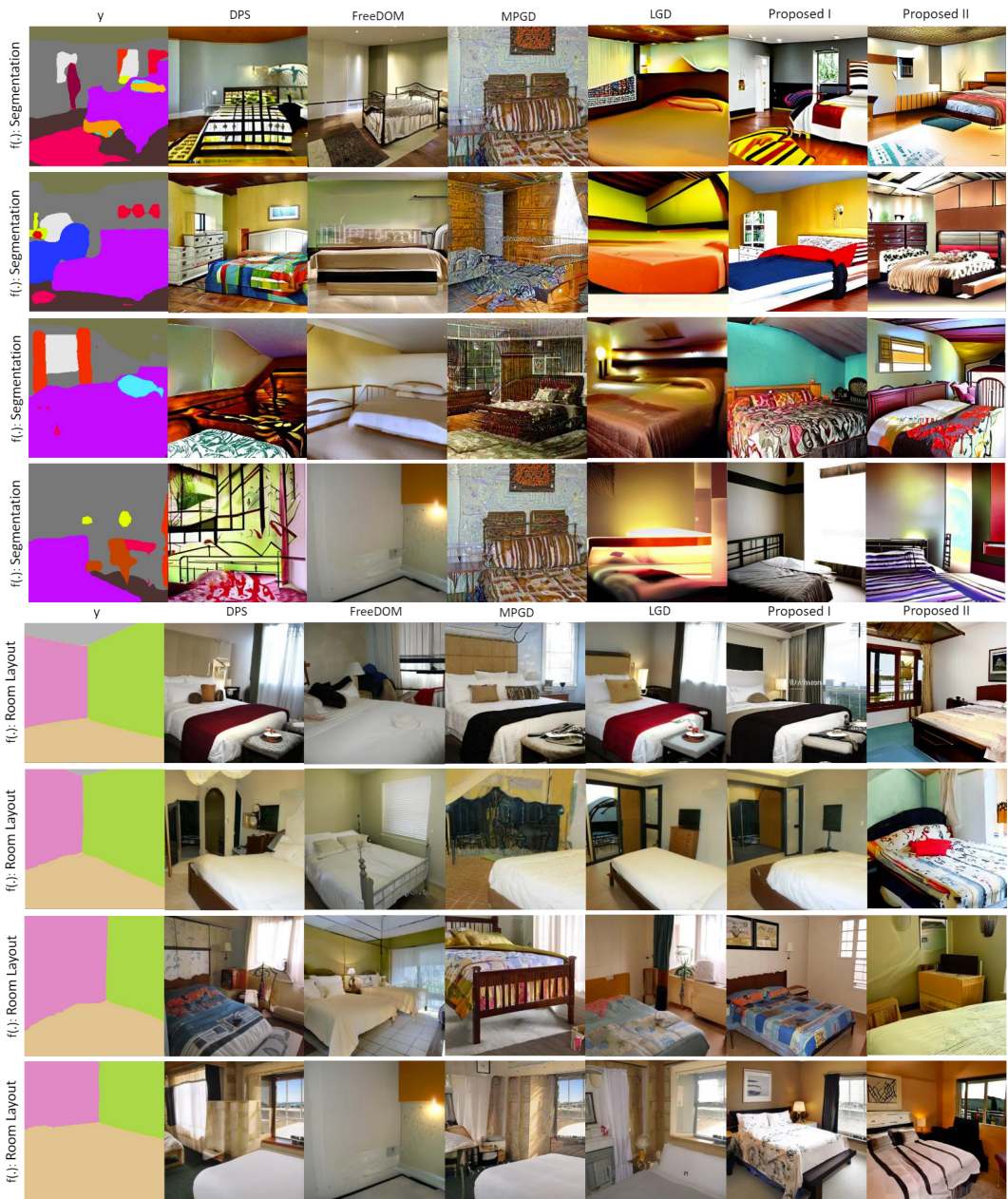


Figure 10: Additional visual results on image segmentation and layout estimation.

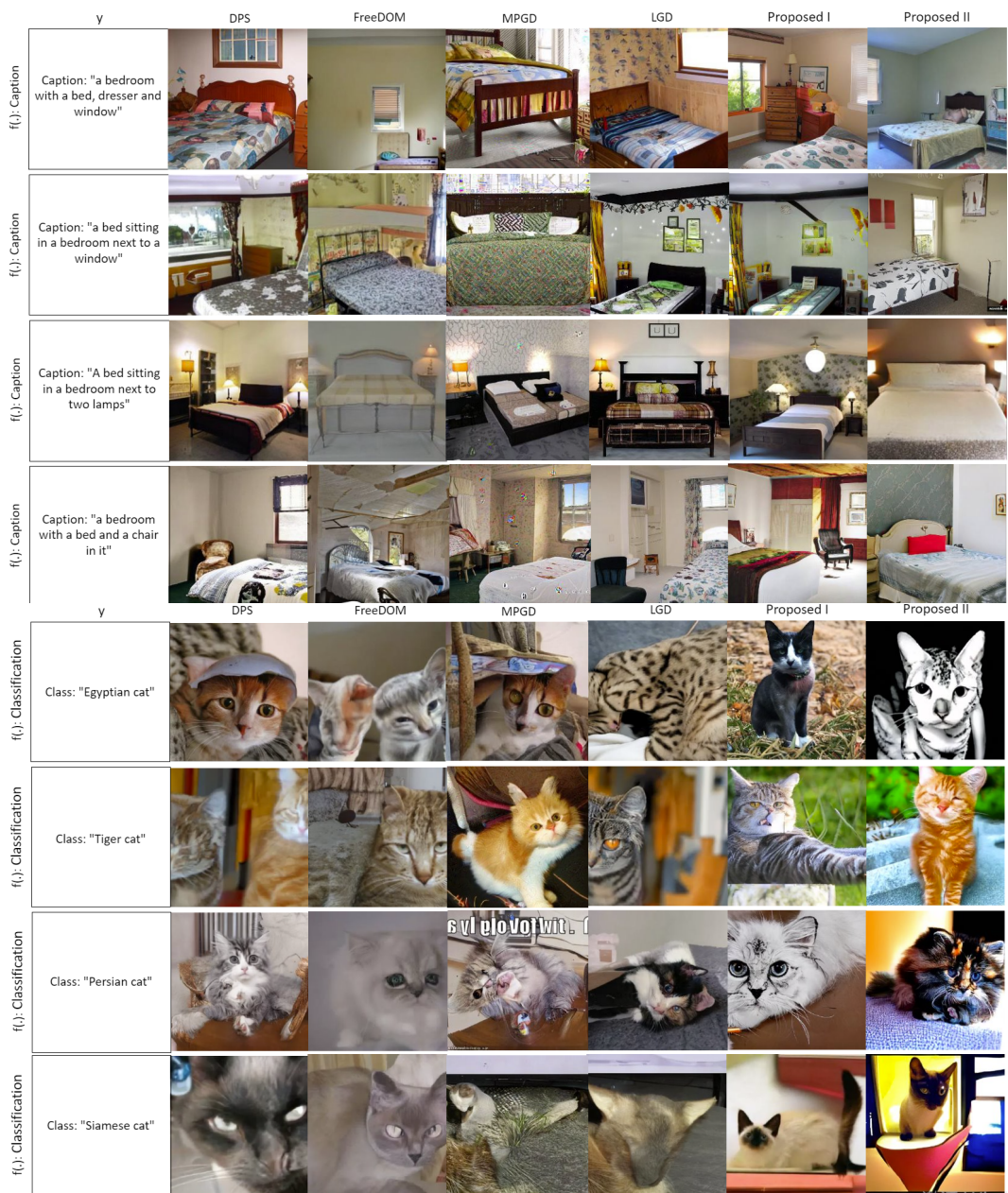


Figure 11: Additional visual results on image captioning and image classification.

NeurIPS Paper Checklist

1. Claims

Question: Do the main claims made in the abstract and introduction accurately reflect the paper's contributions and scope?

Answer: [Yes]

Justification: Yes.

Guidelines:

- The answer NA means that the abstract and introduction do not include the claims made in the paper.
- The abstract and/or introduction should clearly state the claims made, including the contributions made in the paper and important assumptions and limitations. A No or NA answer to this question will not be perceived well by the reviewers.
- The claims made should match theoretical and experimental results, and reflect how much the results can be expected to generalize to other settings.
- It is fine to include aspirational goals as motivation as long as it is clear that these goals are not attained by the paper.

2. Limitations

Question: Does the paper discuss the limitations of the work performed by the authors?

Answer: [Yes]

Justification: In Discussion.

Guidelines:

- The answer NA means that the paper has no limitation while the answer No means that the paper has limitations, but those are not discussed in the paper.
- The authors are encouraged to create a separate "Limitations" section in their paper.
- The paper should point out any strong assumptions and how robust the results are to violations of these assumptions (e.g., independence assumptions, noiseless settings, model well-specification, asymptotic approximations only holding locally). The authors should reflect on how these assumptions might be violated in practice and what the implications would be.
- The authors should reflect on the scope of the claims made, e.g., if the approach was only tested on a few datasets or with a few runs. In general, empirical results often depend on implicit assumptions, which should be articulated.
- The authors should reflect on the factors that influence the performance of the approach. For example, a facial recognition algorithm may perform poorly when image resolution is low or images are taken in low lighting. Or a speech-to-text system might not be used reliably to provide closed captions for online lectures because it fails to handle technical jargon.
- The authors should discuss the computational efficiency of the proposed algorithms and how they scale with dataset size.
- If applicable, the authors should discuss possible limitations of their approach to address problems of privacy and fairness.
- While the authors might fear that complete honesty about limitations might be used by reviewers as grounds for rejection, a worse outcome might be that reviewers discover limitations that aren't acknowledged in the paper. The authors should use their best judgment and recognize that individual actions in favor of transparency play an important role in developing norms that preserve the integrity of the community. Reviewers will be specifically instructed to not penalize honesty concerning limitations.

3. Theory Assumptions and Proofs

Question: For each theoretical result, does the paper provide the full set of assumptions and a complete (and correct) proof?

Answer: [Yes]

Justification: In appendix.

Guidelines:

- The answer NA means that the paper does not include theoretical results.
- All the theorems, formulas, and proofs in the paper should be numbered and cross-referenced.
- All assumptions should be clearly stated or referenced in the statement of any theorems.
- The proofs can either appear in the main paper or the supplemental material, but if they appear in the supplemental material, the authors are encouraged to provide a short proof sketch to provide intuition.
- Inversely, any informal proof provided in the core of the paper should be complemented by formal proofs provided in appendix or supplemental material.
- Theorems and Lemmas that the proof relies upon should be properly referenced.

4. Experimental Result Reproducibility

Question: Does the paper fully disclose all the information needed to reproduce the main experimental results of the paper to the extent that it affects the main claims and/or conclusions of the paper (regardless of whether the code and data are provided or not)?

Answer: [Yes]

Justification: Code is available in supplementary materials.

Guidelines:

- The answer NA means that the paper does not include experiments.
- If the paper includes experiments, a No answer to this question will not be perceived well by the reviewers: Making the paper reproducible is important, regardless of whether the code and data are provided or not.
- If the contribution is a dataset and/or model, the authors should describe the steps taken to make their results reproducible or verifiable.
- Depending on the contribution, reproducibility can be accomplished in various ways. For example, if the contribution is a novel architecture, describing the architecture fully might suffice, or if the contribution is a specific model and empirical evaluation, it may be necessary to either make it possible for others to replicate the model with the same dataset, or provide access to the model. In general, releasing code and data is often one good way to accomplish this, but reproducibility can also be provided via detailed instructions for how to replicate the results, access to a hosted model (e.g., in the case of a large language model), releasing of a model checkpoint, or other means that are appropriate to the research performed.
- While NeurIPS does not require releasing code, the conference does require all submissions to provide some reasonable avenue for reproducibility, which may depend on the nature of the contribution. For example
 - (a) If the contribution is primarily a new algorithm, the paper should make it clear how to reproduce that algorithm.
 - (b) If the contribution is primarily a new model architecture, the paper should describe the architecture clearly and fully.
 - (c) If the contribution is a new model (e.g., a large language model), then there should either be a way to access this model for reproducing the results or a way to reproduce the model (e.g., with an open-source dataset or instructions for how to construct the dataset).
 - (d) We recognize that reproducibility may be tricky in some cases, in which case authors are welcome to describe the particular way they provide for reproducibility. In the case of closed-source models, it may be that access to the model is limited in some way (e.g., to registered users), but it should be possible for other researchers to have some path to reproducing or verifying the results.

5. Open access to data and code

Question: Does the paper provide open access to the data and code, with sufficient instructions to faithfully reproduce the main experimental results, as described in supplemental material?

Answer: [Yes]

Justification: In supplementary materials.

Guidelines:

- The answer NA means that paper does not include experiments requiring code.
- Please see the NeurIPS code and data submission guidelines (<https://nips.cc/public/guides/CodeSubmissionPolicy>) for more details.
- While we encourage the release of code and data, we understand that this might not be possible, so “No” is an acceptable answer. Papers cannot be rejected simply for not including code, unless this is central to the contribution (e.g., for a new open-source benchmark).
- The instructions should contain the exact command and environment needed to run to reproduce the results. See the NeurIPS code and data submission guidelines (<https://nips.cc/public/guides/CodeSubmissionPolicy>) for more details.
- The authors should provide instructions on data access and preparation, including how to access the raw data, preprocessed data, intermediate data, and generated data, etc.
- The authors should provide scripts to reproduce all experimental results for the new proposed method and baselines. If only a subset of experiments are reproducible, they should state which ones are omitted from the script and why.
- At submission time, to preserve anonymity, the authors should release anonymized versions (if applicable).
- Providing as much information as possible in supplemental material (appended to the paper) is recommended, but including URLs to data and code is permitted.

6. Experimental Setting/Details

Question: Does the paper specify all the training and test details (e.g., data splits, hyper-parameters, how they were chosen, type of optimizer, etc.) necessary to understand the results?

Answer: [Yes]

Justification: In Experimental setup and appendix.

Guidelines:

- The answer NA means that the paper does not include experiments.
- The experimental setting should be presented in the core of the paper to a level of detail that is necessary to appreciate the results and make sense of them.
- The full details can be provided either with the code, in appendix, or as supplemental material.

7. Experiment Statistical Significance

Question: Does the paper report error bars suitably and correctly defined or other appropriate information about the statistical significance of the experiments?

Answer: [No]

Justification: Error bar is expensive and rarely reported in our community.

Guidelines:

- The answer NA means that the paper does not include experiments.
- The authors should answer "Yes" if the results are accompanied by error bars, confidence intervals, or statistical significance tests, at least for the experiments that support the main claims of the paper.
- The factors of variability that the error bars are capturing should be clearly stated (for example, train/test split, initialization, random drawing of some parameter, or overall run with given experimental conditions).
- The method for calculating the error bars should be explained (closed form formula, call to a library function, bootstrap, etc.)
- The assumptions made should be given (e.g., Normally distributed errors).
- It should be clear whether the error bar is the standard deviation or the standard error of the mean.

- It is OK to report 1-sigma error bars, but one should state it. The authors should preferably report a 2-sigma error bar than state that they have a 96% CI, if the hypothesis of Normality of errors is not verified.
- For asymmetric distributions, the authors should be careful not to show in tables or figures symmetric error bars that would yield results that are out of range (e.g. negative error rates).
- If error bars are reported in tables or plots, The authors should explain in the text how they were calculated and reference the corresponding figures or tables in the text.

8. Experiments Compute Resources

Question: For each experiment, does the paper provide sufficient information on the computer resources (type of compute workers, memory, time of execution) needed to reproduce the experiments?

Answer: [Yes]

Justification: In Experimental setup and appendix.

Guidelines:

- The answer NA means that the paper does not include experiments.
- The paper should indicate the type of compute workers CPU or GPU, internal cluster, or cloud provider, including relevant memory and storage.
- The paper should provide the amount of compute required for each of the individual experimental runs as well as estimate the total compute.
- The paper should disclose whether the full research project required more compute than the experiments reported in the paper (e.g., preliminary or failed experiments that didn't make it into the paper).

9. Code Of Ethics

Question: Does the research conducted in the paper conform, in every respect, with the NeurIPS Code of Ethics <https://neurips.cc/public/EthicsGuidelines?>

Answer: [Yes]

Justification: Yes.

Guidelines:

- The answer NA means that the authors have not reviewed the NeurIPS Code of Ethics.
- If the authors answer No, they should explain the special circumstances that require a deviation from the Code of Ethics.
- The authors should make sure to preserve anonymity (e.g., if there is a special consideration due to laws or regulations in their jurisdiction).

10. Broader Impacts

Question: Does the paper discuss both potential positive societal impacts and negative societal impacts of the work performed?

Answer: [Yes]

Justification: In appendix.

Guidelines:

- The answer NA means that there is no societal impact of the work performed.
- If the authors answer NA or No, they should explain why their work has no societal impact or why the paper does not address societal impact.
- Examples of negative societal impacts include potential malicious or unintended uses (e.g., disinformation, generating fake profiles, surveillance), fairness considerations (e.g., deployment of technologies that could make decisions that unfairly impact specific groups), privacy considerations, and security considerations.
- The conference expects that many papers will be foundational research and not tied to particular applications, let alone deployments. However, if there is a direct path to any negative applications, the authors should point it out. For example, it is legitimate to point out that an improvement in the quality of generative models could be used to

generate deepfakes for disinformation. On the other hand, it is not needed to point out that a generic algorithm for optimizing neural networks could enable people to train models that generate Deepfakes faster.

- The authors should consider possible harms that could arise when the technology is being used as intended and functioning correctly, harms that could arise when the technology is being used as intended but gives incorrect results, and harms following from (intentional or unintentional) misuse of the technology.
- If there are negative societal impacts, the authors could also discuss possible mitigation strategies (e.g., gated release of models, providing defenses in addition to attacks, mechanisms for monitoring misuse, mechanisms to monitor how a system learns from feedback over time, improving the efficiency and accessibility of ML).

11. Safeguards

Question: Does the paper describe safeguards that have been put in place for responsible release of data or models that have a high risk for misuse (e.g., pretrained language models, image generators, or scraped datasets)?

Answer: [NA]

Justification: No new model is trained.

Guidelines:

- The answer NA means that the paper poses no such risks.
- Released models that have a high risk for misuse or dual-use should be released with necessary safeguards to allow for controlled use of the model, for example by requiring that users adhere to usage guidelines or restrictions to access the model or implementing safety filters.
- Datasets that have been scraped from the Internet could pose safety risks. The authors should describe how they avoided releasing unsafe images.
- We recognize that providing effective safeguards is challenging, and many papers do not require this, but we encourage authors to take this into account and make a best faith effort.

12. Licenses for existing assets

Question: Are the creators or original owners of assets (e.g., code, data, models), used in the paper, properly credited and are the license and terms of use explicitly mentioned and properly respected?

Answer: [Yes]

Justification: In Experimental setup and appendix.

Guidelines:

- The answer NA means that the paper does not use existing assets.
- The authors should cite the original paper that produced the code package or dataset.
- The authors should state which version of the asset is used and, if possible, include a URL.
- The name of the license (e.g., CC-BY 4.0) should be included for each asset.
- For scraped data from a particular source (e.g., website), the copyright and terms of service of that source should be provided.
- If assets are released, the license, copyright information, and terms of use in the package should be provided. For popular datasets, paperswithcode.com/datasets has curated licenses for some datasets. Their licensing guide can help determine the license of a dataset.
- For existing datasets that are re-packaged, both the original license and the license of the derived asset (if it has changed) should be provided.
- If this information is not available online, the authors are encouraged to reach out to the asset's creators.

13. New Assets

Question: Are new assets introduced in the paper well documented and is the documentation provided alongside the assets?

Answer: [Yes]

Justification: In supplementary material

Guidelines:

- The answer NA means that the paper does not release new assets.
- Researchers should communicate the details of the dataset/code/model as part of their submissions via structured templates. This includes details about training, license, limitations, etc.
- The paper should discuss whether and how consent was obtained from people whose asset is used.
- At submission time, remember to anonymize your assets (if applicable). You can either create an anonymized URL or include an anonymized zip file.

14. Crowdsourcing and Research with Human Subjects

Question: For crowdsourcing experiments and research with human subjects, does the paper include the full text of instructions given to participants and screenshots, if applicable, as well as details about compensation (if any)?

Answer: [NA]

Justification: [NA]

Guidelines:

- The answer NA means that the paper does not involve crowdsourcing nor research with human subjects.
- Including this information in the supplemental material is fine, but if the main contribution of the paper involves human subjects, then as much detail as possible should be included in the main paper.
- According to the NeurIPS Code of Ethics, workers involved in data collection, curation, or other labor should be paid at least the minimum wage in the country of the data collector.

15. Institutional Review Board (IRB) Approvals or Equivalent for Research with Human Subjects

Question: Does the paper describe potential risks incurred by study participants, whether such risks were disclosed to the subjects, and whether Institutional Review Board (IRB) approvals (or an equivalent approval/review based on the requirements of your country or institution) were obtained?

Answer: [NA]

Justification: [NA]

Guidelines:

- The answer NA means that the paper does not involve crowdsourcing nor research with human subjects.
- Depending on the country in which research is conducted, IRB approval (or equivalent) may be required for any human subjects research. If you obtained IRB approval, you should clearly state this in the paper.
- We recognize that the procedures for this may vary significantly between institutions and locations, and we expect authors to adhere to the NeurIPS Code of Ethics and the guidelines for their institution.
- For initial submissions, do not include any information that would break anonymity (if applicable), such as the institution conducting the review.